Energy transfer to Gd^{3+} from the self-trapped exciton in $ScPO_4:Gd^{3+}$: Dynamics and application to quantum cutting

Y. Zhou,[1] S. P. Feofilov,[1,*] H. J. Seo,[2] J. Y. Jeong,[3] D. A. Keszler,[3] and R. S. Meltzer[1]
[1]*Department of Physics and Astronomy, University of Georgia, Athens, Georgia 30602, USA*
[2]*Pukyong National University, Busan 608–737, Republic of Korea*
[3]*Department of Chemistry, 153 Gilbert Hall, Oregon State University, Corvallis, Oregon 97331-4003, USA*
(Received 23 October 2007; published 27 February 2008; corrected 3 April 2008)

The dynamics of the host-sensitized excitation of the high-lying ^6G state of Gd^{3+} in $ScPO_4$ is studied as a function of temperature. Excitation of the Gd^{3+} ^6G state has been shown to lead to quantum cutting by photon cascade emission in $ScPO_4$. It is demonstrated that the energy transfer from the self-trapped exciton to Gd^{3+} is thermally activated probably due to exciton mobility. Whereas at low temperatures, energy transfer from the self-trapped exciton (STE) is dominated by transfer to "killer centers," at room temperature the transfer to Gd^{3+} is $>10^{10}$ s^{-1} in samples containing 1% Gd^{3+} and effectively dominates the energy transfer. The experimental results are well described with a model that assumes two STE states split by 280 cm^{-1}, a lower triplet and an upper singlet, whose radiative rates differ by about 2 orders of magnitude. The comparison with the model yields a thermal activation energy of 980 cm^{-1}. Sensitization using the host excitations therefore seems like a promising route to promote quantum cutting with Gd^{3+} but hosts with STE emission at or below 200 nm are necessary for improved quantum yields.

DOI: 10.1103/PhysRevB.77.075129 PACS number(s): 78.47.−p, 71.35.Aa, 78.55.Hx

INTRODUCTION

In order to reduce society's consumption of energy, there is great interest in improving the efficiency of light sources. In addition, mercury, which provides the initial ultraviolet light source in fluorescent lamps, acts as a pollutant during the disposal of these lamps. This has led to an increased interest in the process of quantum cutting, whereby one high energy photon is converted into two or more lower energy photons in the visible. In such a device, mercury would be replaced by a noble gas such as xenon for the lamp discharge. Indeed it is the xenon discharge that is the basis of plasma displays. Since xenon emits in the vacuum ultraviolet (VUV), the energy loss in converting a VUV photon to one visible photon is too large to make such lamps as energy efficient as current fluorescent lamps. However, quantum cutting could solve this problem, motivating a search for phosphors with good quantum cutting efficiencies under VUV excitation.

Quantum cutting has been demonstrated based on three different mechanisms. Several reviews of the subject of quantum cutting are available in the literature.[1–3] The initial demonstration involved photon cascade emission (PCE) occurring in $YF_3:Pr^{3+}$.[4,5] In this case, the Pr^{3+} was excited to its $4f5d$ state in a strong parity allowed transition. Rapid relaxation to the $^1S_0$ state of the $4f^2$ configuration was followed by two successive radiative transitions yielding ideally two photons emitted for one VUV photon absorbed. The measured quantum efficiency was about 127%.[6] Quantum cutting with internal quantum efficiency of 190% has been demonstrated in $LiGdF_4:Eu$ using a second mechanism, cross relaxation energy transfer.[7] After excitation of the ^6G state of Gd^{3+} at an energy of about 50 000 cm^{-1}, a nonradiative cross relaxation energy transfer process occurs whereby the Gd^{3+} ion undergoes a transition to its ^6P state while the Eu^{3+} ion is excited from its thermally populated (at room temperature) $^7F_1$ low-lying level to the $^5D_0$ state. Both ions then radiate photons with high efficiency yielding the high internal quantum yield. A third possibility involves Auger processes in which the initial photon is capable of generating a number of free electrons which can each excite a radiative center.

Photon cascade emission has also been demonstrated for the Gd^{3+} ion in $GdLiF_4$,[8] $GdBaB_9O_{16}$,[9] and $ScPO_4$.[10] In this case, Gd^{3+} radiates in a sequential two step process; the first transition is $^6G \rightarrow {}^6P$ in the red followed by a $^6P \rightarrow {}^8S$ transition in the UV. However, a second ion can be introduced so that an energy transfer occurs from the ^6P state of Gd^{3+} to this second ion which can emit a visible photon. Thus Gd^{3+} offers a number of opportunities for the development of quantum cutting phosphors. However, the practical use of PCE for Gd^{3+} has been limited by the inability to efficiently excite the ^6G state of Gd^{3+} since transitions to this state from its ground state are parity forbidden ($4f^7 \rightarrow 4f^7$) and the $4f^6 5d$ state lies at too high an energy to be accessible with a xenon discharge. Attempts have been made by sensitizing Gd^{3+} with other rare earth ions that have $5d$ states such that they can be excited by the xenon discharge, but none of these have provided the required efficiencies.[11–13] In a previous paper,[10] we showed that the self-trapped exciton (STE) can be used to sensitize the ^6G state of Gd^{3+} but the quantum efficiency was only about 100% under 170 nm excitation, not the desired 200%. The problem lies in part to the fact that 75% of the energy flows to the lower-lying ^6D and ^6I states of Gd^{3+} which cannot produce visible quantum cutting. It is the purpose of this paper to examine in detail the STE $\rightarrow Gd^{3+}$ (^6G) energy transfer process, especially the dynamics and its temperature dependence, so as to better understand this process in order that we might evaluate it and optimize it for sensitizing the ^6G state of Gd^{3+}. More generally, these results should be of relevance to the use of the STE as a sensitizing agent.

EXPERIMENT

The preparation of these samples of doped and undoped $ScPO_4$ has been described previously.[10] A powder sample was placed in a 0.5 mm deep pocket of a cold finger that was covered by a MgF_2 window. The cold finger was placed in a vacuum chamber. Its hollow core could be filled with liquid nitrogen for the lowest temperatures. Higher temperatures were obtained during the warming cycle after the liquid nitrogen was exhausted. A thermocouple attached to the cold finger registered the temperature. A radiation shield, attached to the cold finger at its upper end and surrounding the sample, reduced the room temperature radiation from reaching the sample and thereby helped us to maintain the temperature of the powder close to that of the thermocouple.

Emission spectra were obtained by exciting the sample, contained in vacuum, either with a deuterium lamp, spectrally filtered with an Acton VM-502 VUV monochromator, or with a model EX5 GAM pulsed laser (pulse width of 10 ns) operating at 157 nm. The visible and UV emission was dispersed with an Acton Spectrapro-150 spectrometer and was detected with a Santa Barbara Instrument Group ST-6I charge-coupled device camera. All emission spectra were corrected for the wavelength-dependent response of the detection system.

For the time-resolved data, the samples were excited with the model EX5 GAM pulsed laser (pulse width of 10 ns) operating at 157 nm. The laser emission was passed through an Acton Research VUV 157 nm interference filter in order to eliminate other wavelengths from the emission of the laser discharge. The emission was selected with a 0.25 m monochromator and additional colored glass or interference filters. The bandwidth of the instrument was ~3 nm. The emission was detected with a photomultiplier tube and was averaged and stored in a digital oscilloscope. A temporal resolution of about 5 ns was obtained.

TEMPERATURE DEPENDENCE OF THE EMISSION

$ScPO_4$ has a STE emission that peaks at 220 nm, one of the shortest known STE emissions. Only some fluorides and a few oxides such as Al_2O_3 show STE emission at shorter wavelengths. The emission spectrum of an undoped and a 1% Gd^{3+}-doped $ScPO_4$ sample at 300 K is shown in Fig. 1. The Gd^{3+} transitions which appear in Fig. 1 are identified on the energy level diagram in Fig. 2. Also shown schematically in Fig. 2 are the initial *e-h* pair and the relaxed STE state. After creation of the *e-h* pair by the absorption of the VUV photon in an above band gap transition, an exciton is formed which becomes self-trapped as a STE. When Gd^{3+} is introduced, an energy transfer occurs from the STE to the excited states of Gd^{3+}, as shown in Fig. 2. In the presence of Gd^{3+}, the STE emission is almost totally quenched with the appearance of ^6G state emission from Gd^{3+}, along with emission from the ^6P state. This replacement of the STE emission with ^6G emission of Gd^{3+} strongly suggests a STE$\rightarrow Gd^{3+}$ energy transfer involving the ^6G state. The spin-allowed Gd^{3+} transitions from ^6G are much stronger than the spin-forbidden transitions. However, the much higher transition

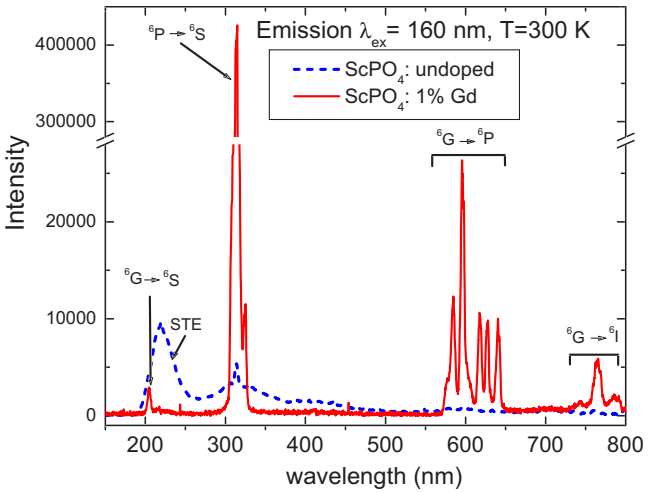

FIG. 1. (Color online) Emission spectra excited at 160 nm of undoped and 1% Gd-doped $ScPO_4$ at $T=300$ K. The Gd^{3+} transitions and the STE are identified.

energy of the spin-forbidden transition to the ground state at 204 nm partially compensates for its spin-forbidden character as the radiative rates are proportional to the cube of the transition frequency. As a result it retains considerable intensity.

When the sample containing 1% Gd^{3+} is cooled to 77 K, the STE emission, which had almost vanished due to the Gd^{3+} doping at 297 K, increases in intensity and is again clearly observed. This is shown in Fig. 3 which compares the 77 and 297 K spectra. Along with a decrease in the STE emission in going from 77 to 297 K, the Gd^{3+} ^6G emission intensity increases. These facts suggest an increased efficiency of the STE$\rightarrow Gd^{3+}$ energy transfer as the temperature is raised. Presumably this implies an energy transfer rate that increases with temperature. The temperature dependence of the luminescence is shown in detail in Fig. 4 for both the undoped and 1% Gd^{3+} samples. Even the undoped sample

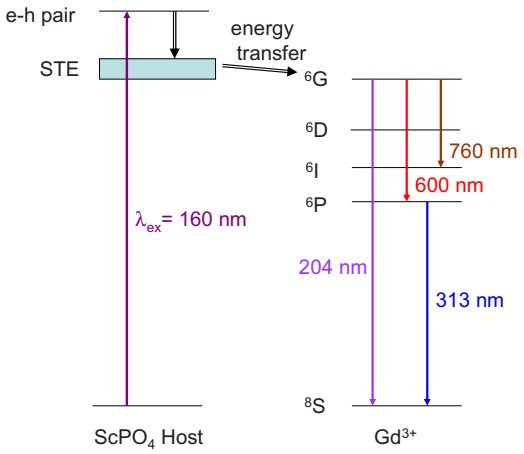

FIG. 2. (Color online) Schematic showing the creation of the initial *e-h* pair, the relaxation to form the STE, and the subsequent energy flow to the excited states of Gd^{3+}. The relevant energy levels of Gd^{3+}, along with the Gd^{3+} transitions observed in Fig. 1, are identified.

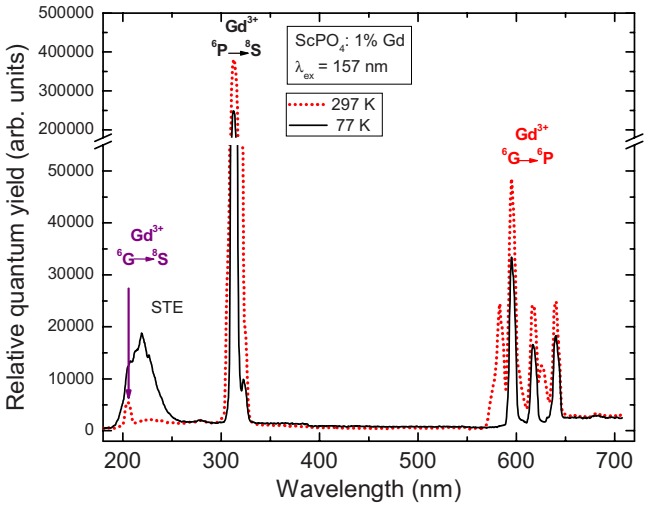

FIG. 3. (Color online) Emission spectra excited at 157 nm of 1% Gd-doped $ScPO_4$ at T=77 and 297 K.

exhibits a STE intensity that decreases with an increase in temperature. This likely results from a thermally activated quenching process such as an intrinsic quenching of the STE or a partial energy transfer to nonradiative "killer centers" due to the presence of defects or impurities. For the 1% Gd^{3+} sample the temperature dependence of the STE emission is much stronger, nearly totally quenching the STE emission at room temperature. It appears that the energy transfer to the Gd^{3+} ions dominates over the other quenching processes in the Gd^{3+}-doped material.

TEMPERATURE DEPENDENCE OF THE SELF-TRAPPED EXCITON EMISSION DYNAMICS

We showed previously that at room temperature the lifetime of the STE emission shortens from 75 ns in the undoped sample to 8 ns in the sample containing 1% Gd^{3+}.[10] While it was previously not possible for us to obtain the ^6G buildup rate, this information will be presented in the next section. This observation is consistent with a strong energy transfer from the STE to Gd^{3+}. We also measured a STE decay time of 130 ns at 300 K in a single crystal of $ScPO_4$. The longer lifetime in the single crystal tells us that in our powders (and perhaps also the crystal) this is not the radiative lifetime, a fact that is not surprising in the presence of energy transfer to killer centers. We now examine the temperature dependence of the dynamics to help us identify the energy transfer processes and to determine their mechanisms.

The time dependence of the STE emission as a function of temperature after pulsed excitation at 157 nm in both the undoped sample measured at 240 nm (upper) and doped sample measured at 220 nm (lower) is shown in Fig. 5. For the undoped sample, there is a striking increase in the lifetime as the temperature is reduced, reaching 2.5 μs at 77 K. One also notices a decrease of the initial intensity of the STE at the lowest two measured temperatures. This means either that the radiative rate of the STE noticeably decreases below about 150 K or that the efficiency for the creation of the STE decreases at the lower temperatures. We think that the latter

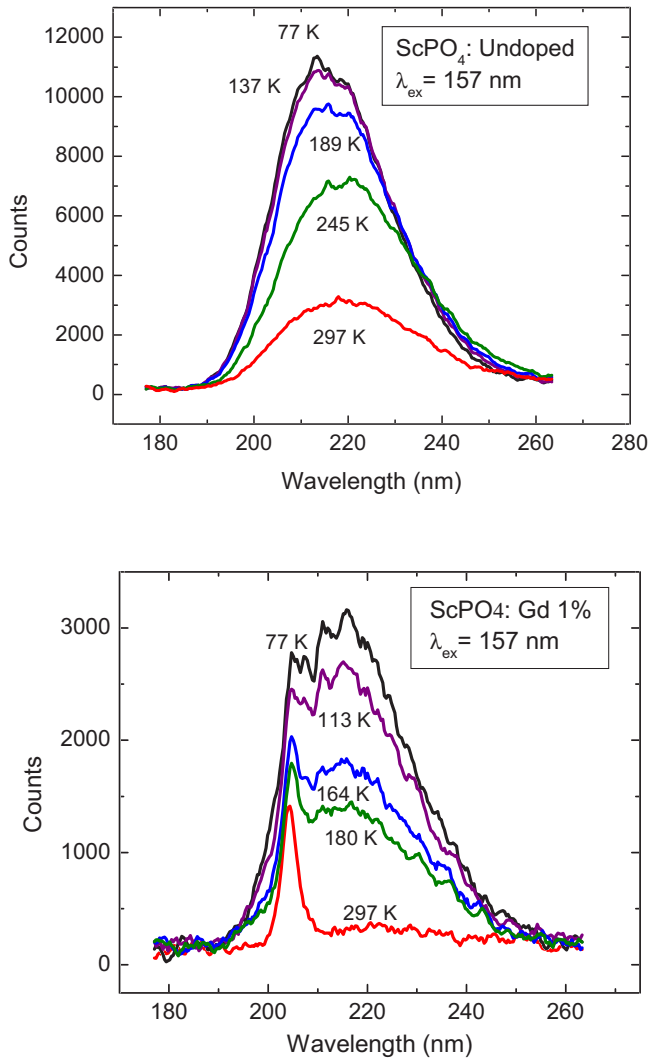

FIG. 4. (Color online) vuv emission spectra excited at 157 nm of undoped (upper) and 1% Gd-doped (lower) $ScPO_4$ as a function of temperature.

is unlikely and that the reduced initial intensity results from a reduction of the radiative rate for reasons that will be discussed below. A similar reduction in initial intensity is seen for the 1% Gd^{3+} sample. In this sample, the temperature dependence is much more dramatic. At 77 K, the STE lifetime is nearly identical in the two samples. This suggests that at 77 K the STE$\rightarrow Gd^{3+}$ energy transfer no longer competes with the radiative rate and has thus become unimportant in determining the STE luminescence dynamics. The lifetime is therefore dominated by the radiative rate and is nearly the same in both samples. However, since the radiative rate is temperature dependent, we assume that there are two STE excited states with two different radiative rates, whose relative populations are of course temperature dependent.

MODEL FOR THE LUMINESCENCE DYNAMICS

In order to explain the temperature dependence of both the intensity and decay rate of the STE we propose the following model schematically outlined in Fig. 6. We assume

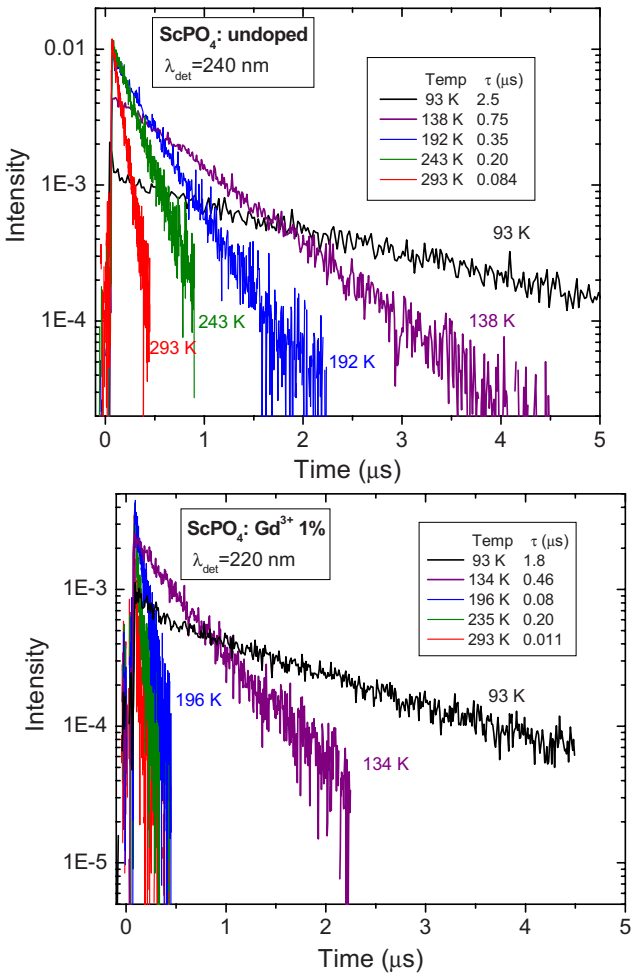

FIG. 5. (Color online) Time dependence of the emission, excited at 157 nm, of undoped (upper) and 1% Gd-doped $ScPO_4$ (lower) as a function of temperature. The legend shows the best exponential fits of the decay of the data.

two STE states, STE 1 and STE 2, with very different radiative rates. Their populations are N_1 and N_2, respectively. These might arise from the high spin and low spin STEs arising from the two possible relative spin orientations for the exciton electron-hole pair, as observed in the alkali

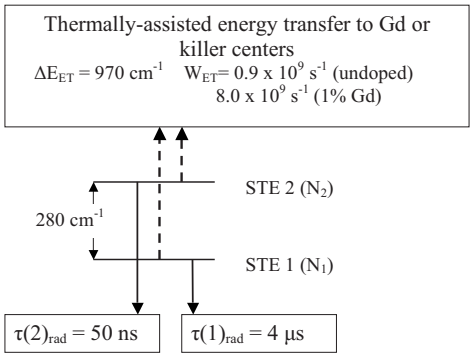

FIG. 6. Schematic indicating the model used to fit the temperature dependence of the rates and normalized integrated emission intensities of undoped and 1% Gd-doped $ScPO_4$. The numbers are the values of the best fits shown in Fig. 7.

halides.[14] In this model, the triplet lies lowest with a smaller radiative rate of $\tau(1)_{\mathrm{rad}}^{-1}$ while the singlet, lying at an energy Δ higher in energy, has a much larger radiative rate $\tau(2)_{\mathrm{rad}}^{-1}$. Alternatively the STE may have many excited states as seen in $PbWO_4$ where the splitting between the lowest two STE excited states is 1044 cm^{-1}.[15] For a 1% Gd concentration it is statistically unlikely that the STE will be created close to a Gd. Therefore, at low temperature, when the STE is localized, the energy transfer rate to Gd^{3+} is sufficiently reduced such that it is relatively unimportant in controlling the emission dynamics. As the temperature is raised, the STE becomes mobile and a thermally assisted energy transfer process is activated with an activation energy of ΔE_{ET}, increasing the probability that the STE and Gd^{3+} will be proximate for a portion of the time. Although the energy transfer consists of two steps, the energy migration of the STE to the vicinity of the Gd^{3+} followed by energy transfer to the Gd^{3+}, each with their own activation energy,[16] we assume that one of these is much faster so that the other is the rate-limiting process at all experimentally observed temperatures. The above statement also applies to the energy transfer to the killer centers. We note that self-quenching of the STE emission is a possible alternative to quenching by killer centers. While it is not possible to eliminate this possibility, the fact that the data can be fitted with a single activation energy for both the STE$\rightarrow Gd^{3+}$ energy transfer and the quenching process in the undoped materials suggests that it is the exciton mobility that dominates the dynamics at higher temperatures, not the self-quenching. Furthermore, in order to keep the model relatively simple, we also assume the same activation energy and energy transfer rate from both STE states. These assumptions turn out to be adequate to explain the experimental results.

In such a model, the STE decay rate can be expressed as

$$\tau_{\mathrm{STE}}^{-1} = \tau_{\mathrm{rad}}^{-1} + \tau_{\mathrm{ET}}^{-1} = N_1 \tau(1)_{\mathrm{rad}}^{-1} + N_2 \tau(2)_{\mathrm{rad}}^{-1} + W_{\mathrm{ET}} \exp(-\Delta E_{\mathrm{ET}}/\mathrm{kT}), \quad (1)$$

where $N_2/N_1 = \exp(-\Delta/kT)$. τ_{ET}^{-1} includes energy transfer to both Gd^{3+} and killer centers and any other intrinsic STE quenching processes. Here, W_{ET} is the frequency factor for the energy transfer. The integrated STE intensity will be proportional to the product of the radiative rate and the lifetime according to

$$I_{\mathrm{STE}} \alpha \tau_{\mathrm{rad}}^{-1} \tau_{\mathrm{STE}}. \quad (2)$$

In Fig. 7, we compare the results of the model to the experimental data for both the STE decay rate and the normalized STE intensity. The open circles and squares refer to the experimentally determined decay rates of the undoped and 1% Gd-doped samples, respectively. The symbols X and + refer to the observed normalized STE intensity of the undoped and 1% Gd-doped samples, respectively. Also shown with the symbol Δ is the buildup rate of the ^6P Gd^{3+} emission. It is close to the decay rate of the STE at all but the lowest temperatures. The rate equations for the model were solved as the parameters in the model were varied so as to provide a best fit to both the temperature dependence of the STE decay rate and intensity. The best fit, shown by the solid

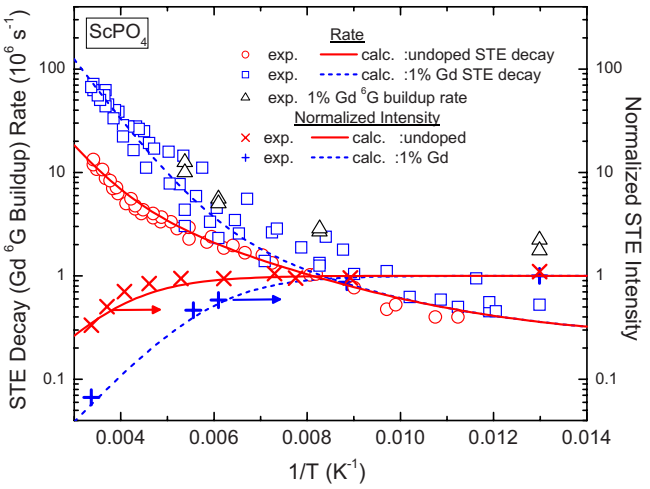

FIG. 7. (Color online) Comparison of the data to the best fits of the model shown in Fig. 6 for the rates and normalized integrated intensities as a function of temperature for the undoped and 1% Gd-doped $ScPO_4$.

and dashed lines in Fig. 7, describes the main features of the temperature dependence. The resulting best fit parameters are given on Fig. 6. Note the W_{ET} is about an order of magnitude higher in the Gd-doped samples indicating that the energy transfer rate to Gd is about ten times higher than the rate to the killer centers for a 1% Gd^{3+} concentration. The two STE states are split by about 280 cm^{-1} and the radiative rate of the upper STE state is about 2 orders of magnitude greater than that of the lower. The thermal activation energy for energy migration is about the energy of one optical phonon in this lattice.

CONCLUSIONS

Sensitization of the ^6G state of Gd^{3+} by energy transfer from the self-trapped exciton has been demonstrated and its dynamics has been determined. As shown previously, the efficiency of energy transfer to the ^6G state is only about 30%, limiting the usefulness of this material as a quantum splitting phosphor.[10] At room temperature the energy transfer to Gd^{3+} ions is highly efficient competing effectively with both radiative decay of the STE and the combination of intrinsic quenching of the STE and energy transfer to killer centers. A rate equation model describes the dynamics quite well. The model assumes two STE states split by 280 cm^{-1}, whose radiative rates differ by about 2 orders of magnitude. A comparison of the model with the experimentally measured temperature dependence of both the dynamics and emission intensity allows for a detailed study of the thermally activated energy transfer and a determination of the activation energy as 970 cm^{-1}.

To use STE sensitization of the ^6G state of Gd^{3+} for quantum cutting, it will be necessary to identify materials whose STE emission occurs at even shorter wavelengths than is the case for $ScPO_4$ so that a larger fraction of the energy transfer occurs to the ^6G state or even higher-lying states of Gd^{3+}. Results of this study, however, do demonstrate that sensitization with the STE is a very effective means of obtaining good coupling of the VUV excitation to Gd^{3+}.

ACKNOWLEDGMENTS

We appreciate the financial support of the U.S. National Science Foundation, Grant Nos. 0305400 (R.S.M.) and 0305449 (D.A.K.). The single crystal of undoped $ScPO_4$ was kindly supplied by Lynn Boatner of Oak Ridge National Laboratory.

*Permanent address: A.F. Ioffe Physical-Technical Institute, 194021 St. Petersburg, Russia.

[1] C. Ronda, J. Lumin. **100**, 301 (2002).
[2] A. Lushchik, C. Lushchik, A. Kotlov, I. Kudryavtseva, A. Maaroos, V. Nagirnyi, and E. Vasil'chenko, Radiat. Meas. **38**, 747 (2004).
[3] R. S. Meltzer, in *Practical Applications of Phosphors*, edited by W. M. Yen, S. Shionoya, and H. Yamamoto (CRC, Boca Raton, FL, 2007), Chap. 2.8, pp. 167–191.
[4] W. W. Piper, J. A. de Luca, and F. S. Ham, J. Lumin. **8**, 344 (1974).
[5] J. I. Sommerdijk, A. Bril, and A. W. de Jager, J. Lumin. **8**, 341 (1974).
[6] A. Kuck, I. Sokolska, M. Henke, and E. Osiac, Chem. Phys. **310**, 139 (2005).
[7] R. T. Wegh, H. Donker, K. Oskam, and A. Meijerink, Science **283**, 663 (1999).
[8] R. T. Wegh, H. Donker, A. Meijerink, R. J. Lamminmaki, and J. Holsa, Phys. Rev. B **56**, 13841 (1997).
[9] Z. Yang, H. H. Lin, M. Z. Su, Y. Tao, and W. Wang, J. Alloys Compd. **308**, 94 (2000).
[10] S. P. Feofilov, Y. Zhou, H. J. Seo, J. Y. Jeong, D. A. Keszler, and R. S. Meltzer, Phys. Rev. B **74**, 085101 (2006).
[11] R. T. Wegh, E. V. D. van Loef, and A. Meijerink, J. Lumin. **90**, 111 (2000).
[12] P. S. Peizel, W. J. M. Schrama, and A. Meijerink, Mol. Phys. **102**, 1285 (2004).
[13] W. Jia, Y. Zhou, S. P. Feofilov, R. S. Meltzer, J. Y. Jeong, and D. Keszler, Phys. Rev. B **72**, 075114 (2005).
[14] R. T. Williams and K. S. Song, J. Phys. Chem. Solids **51**, 679 (1990) and references therein.
[15] M. Itoh and T. Sakurai, Phys. Status Solidi B **242**, R52 (2005).
[16] G. Bizarri and P. Dorenbos, Phys. Rev. B **75**, 184302 (2007).